An-Najah University Journal for Research – A
Natural Sciences

Assessing the impact of climate change in Iraq using the heat index and standardized temperature index

Anas Mahmood Al-Juboori [1]*, Mustafa Salim Mustafa[1], Basma Al-Jawadi[1]

Type: Full Article. Received: 20th April 2026, Accepted: 16th July 2026

Accepted Manuscript, In Press

Abstract: Iraq is experiencing a significant rise in temperatures and frequent heat waves, increasing exposure to heat stress due to these extreme temperatures. This study provides a comprehensive analysis of temperature variations in Iraq using two temperature indices: the standardized temperature index and the heat index, in addition to a spatial analysis of heat stress using a geographic information system (GIS). Air temperature and relative humidity data on a daily timescale for the period 1981-2024 from NASA POWER (Prediction of Worldwide Energy Resources) were used. The results clearly demonstrate the impact of rising temperatures resulting from climate change. Trend analysis of the heat index indicated a significant increase in heat stress across Iraq. Furthermore, the spatial analysis of the heat index showed a significant increase in extreme index values, confirming that northern Iraq is more affected by climate change than other regions. In this study, a mathematical equation was developed to estimate the heat index using gene expression programming to reduce the steps and time required to calculate the heat index using traditional methods. The equation proved its efficiency, as the value of the coefficient of determination was 0.99 in the training phase and 0.98 in the model validation phase.

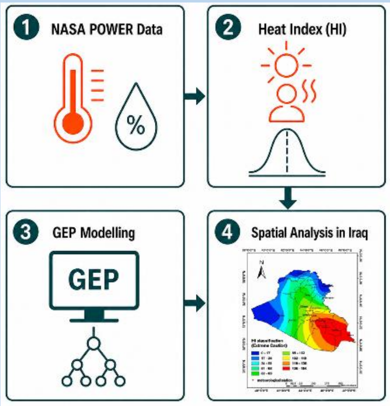

Keywords: Heat index, standardized temperature index, climate change, Environmental sustainability, Extreme heat events, GEP, GIS.

Introduction

Climate change is intensifying the frequency, duration, and severity of extreme heat events, making heat one of the most important weather-related hazards for human health, ecosystems, and economies worldwide. Rising global mean temperatures, coupled with changes in humidity patterns, have increased the number of days with potentially dangerous thermal conditions in many regions, particularly in urban areas and developing countries with limited adaptive capacity [1]. In such contexts, extreme heat not only increases the risk of heat-related illness and death, but also exacerbates energy demand, degrades outdoor labor productivity, and stresses critical infrastructure [2,3]. Consequently, understanding how heat-related indices evolve over time has become central to climate risk assessment and adaptation planning [4].

Traditional indicators of climate change, such as mean air temperature, maximum daily temperature, and heatwave counts, provide essential information about warming trends but can be insufficient to describe how heat is actually experienced by humans [5]. These metrics typically overlook the combined role of temperature and atmospheric moisture in shaping human thermal stress, even though humidity strongly influences evaporative cooling from the skin and thus the body's ability to regulate internal temperature [6]. In humid climates or during moist heat events, relatively moderate air temperatures can still result in severe physiological stress because sweat evaporation is inhibited, leading to a higher perceived temperature than indicated by dry-bulb measurements alone. This gap has motivated growing interest in bioclimatic and biometeorological indices that integrate multiple atmospheric variables to more accurately represent human-experienced heat [7].

In recent decades, the world has witnessed a significant rise in temperatures due to global warming and climate change, exacerbating environmental and health problems and leading to dire consequences for human health [8]. Iraq is among the countries most affected by climate change, having recorded unprecedented record temperatures in recent years [9]. This marked increase in temperatures has intensified the heat stress already experienced by the population [10]. The use of heat indices is one of the methods used in analyzing heat stress and showing how heat stress affects humans [11].

A growing body of research has documented rising heat stress under climate change in many regions, including the Mediterranean basin, East and Southeast Asia, and at the global scale. These studies consistently show increases in the frequency, intensity, and duration of dangerous heat conditions, often emphasizing the combined role of temperature and humidity and, more recently, compound heat–precipitation extremes. However, most of this work has focused on other

[1] Dams and Water Resources Research Center, University of Mosul, Mosul, Iraq
*Corresponding author e-mail: anasmmr@uomosul.edu.iq : ORCID ID: 0000-0002-0206-6324

regions and has not examined in detail how human-perceived heat stress is evolving across Iraq's diverse climatic zones [12–17].

In [18], a new method is proposed for calculating the Wet Bulb Globe Temperature (WBGT), a widely used heat stress index, to overcome the problem of sparse observations of globe and wet-bulb temperature that hinder accurate WBGT estimation, while [19] examines four decades of Universal Thermal Climate Index (UTCI) changes across the Middle East and North Africa (MENA), revealing an accelerating rise in human heat stress with pronounced hotspots in eastern Saudi Arabia, much of Iraq and Syria, and parts of North and West Africa; building on this, [20] highlights that climate change is already inflicting severe environmental and socio-economic damage in Iraq, particularly through increasing water scarcity, land degradation, and escalating human and ecological crises. Complementing this, and [21] synthesizes evidence that the Eastern Mediterranean and Middle East (EMME) has emerged as a major global climate-change hotspot, warming nearly twice as fast as the global mean and experiencing rapidly increasing extreme events, dust, and related socio-economic risks under continued greenhouse gas emissions.

For Iraq, previous studies have demonstrated pronounced warming, increased drought, and expanding desertification, confirming that the country is highly vulnerable to climate change. Yet, there remains a lack of comprehensive assessments that quantify human-perceived heat stress using combined temperature–humidity indices and that compare these metrics across Iraq's northern, central, and southern regions. In particular, few studies have simultaneously applied the heat index (HI) and a standardized temperature index (STI), integrated trend analysis, and explored data-driven equations for heat-index estimation. Recent international assessments indicate that Iraq is among the countries most vulnerable to the impacts of climate change, including extreme heat, drought, and water scarcity.

Traditional heat index calculations, which use maximum daily temperature data and are commonly employed in the medical field to determine the impact of maximum daily temperature on human health on a given day, do not provide an accurate picture of the hydrological impact of climate change on heat. In this study, the average daily heat index will be used instead of the maximum daily heat index to assess heat stress in Iraq as a case study. This is because the average daily heat index reflects the impact of daily temperature and humidity on the heat index for the entire day, thus contributing to the analysis of climate change and facilitating comparison with other indices, such as the STI. Furthermore. A gene expression programming algorithm will be used to develop a mathematical equation for estimating the heat index easier than the traditional equations used to calculate the heat index.

Study area and data

The study area covers the entire territory of Iraq, represented by 21 reference locations corresponding to national meteorological stations distributed across all Iraqi governorates. Mean daily and monthly air temperature (ºC) and relative humidity (%) for the period 1981–2024 were obtained from the Prediction of Worldwide Energy Resources (POWER) project of the National Aeronautics and Space Administration (NASA) via the NASA POWER data access system [22]. For each station coordinate, the corresponding NASA POWER grid-cell values were extracted, representing satellite-driven reanalysis of meteorological data. The spatial distribution of the 21 station locations (POWER grid points) is shown in Figure 1.

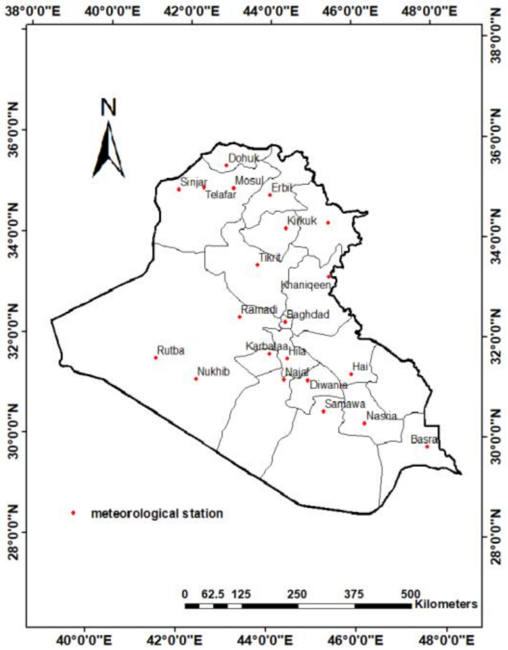

Figure 1: Map of Iraq and locations of meteorological stations

The NASA POWER meteorological data were used in [23] against observations from 10 Iraqi stations over 12 years for temperature, rainfall, wind speed, solar radiation, and relative humidity. The study has managed to showcase a high degree of accuracy for temperature (with a correlation close to 0.75–0.91) and strong to very strong correlations for radiation using Kendall's Tau and mean bias error. The same lends credence to its applicability in solar assessments. The weak to moderate correlations between rainfall and wind suggest that NASA POWER can be used as a supplementary source but have to be calibrated.

In general, NASA POWER is a reliable source but should be validated for specific applications and regions in Iraq. Table 1 presents daily temperature and relative humidity statistics for the meteorological station considered in this study.

Heat index (HI)

The heat index indicates how hot and humid air feels when temperature and humidity are combined. For example, at the same temperature, high humidity reduces the body's ability to cool naturally and increase the perceived temperature because high humidity makes it harder for sweat to evaporate. The heat index helps identify conditions that lead to heat stress in humans. It is calculated using regression equations developed by the National Weather Service (NWS) in 1990, known as the Rothfusz equation (Eq. 1).

$$\begin{aligned} HI = & -42.379 + 2.04901523T + 10.14333127RH \\ & - 0.22475541T \times RH - .00683783T^2 \\ & - 0.05481717RH^2 + 0.00122874T^2 \times RH \\ & + 0.00085282T \times RH^2 \\ & - 0.00000199T^2 \times RH^2 \qquad (1) \end{aligned}$$

The variables are defined as follows: T represents daily temperature in degrees Fahrenheit, RH indicates relative humidity in percent, and HI refers to the heat index, which is the apparent temperature also measured in degrees Fahrenheit. If the relative humidity is under 13% and the temperature falls between 80- and 112-degrees Fahrenheit, the following adjustment will be subtracted from heat index (Eq. 2).

$$Adjustment = \frac{13 - RH}{4} * \sqrt{17 - \left|\frac{T - 95}{17}\right|} \qquad (2)$$

If the relative humidity exceeds 85% and the temperature falls between 80 to 87 degrees Fahrenheit, then the following adjustment is added to heat index (Eq. 3).

$$Adjustment = \left(\frac{RH - 85}{10}\right)\left(\frac{87 - T}{5}\right) \qquad (3)$$

The Rothfusz equation is not appropriate when temperature is equal or below 80 degrees Fahrenheit. In those cases, the following formula is used to calculate the heat index (Eq. 4).

$$HI = 0.5\big(T + 61 + 1.2(T - 68) + (0.094RH)\big) \qquad (4)$$

To calculate the monthly heat index, the daily heat index is first calculated, and then the monthly average is calculated for each month of the year. Table 2 shows the heat index classifications. Visual Basic program was developed to calculate the heat index and make all necessary adjustments in case of low or high relative humidity according to the conditions (temperature, relative humidity) specified by the National Weather Service.

Table 1. Daily temperature and relative humidity statistics for the studied meteorological stations.

Station name	Temperature (°F)			
	Min.	**Max.**	**Mean**	**SD**
Baghdad	33.3	110.0	74.8	18.88
Basra	36.4	111.8	79.2	18.32
Diwania	32.5	109.9	75.4	18.76
Dohuk	15.1	98.0	62.1	20.81
Erbil	25.6	105.0	69.4	19.24
Al-Hai	35.4	111.8	78.0	19.08
Hila	33.8	110.2	75.8	18.94
Karbalaa	33.0	107.5	74.4	19.00
khaniqen	27.6	103.9	70.1	18.77
Kirkuk	25.4	106.4	69.9	19.09
Mosul	25.1	105.3	68.2	19.39
Najaf	33.7	110.1	76.1	19.20
Nasirya	35.7	111.5	78.7	18.96
Nukhib	31.2	105.9	72.2	18.79
Ramadi	32.5	106.3	73.2	18.71
Rutba	23.8	103.3	69.1	19.11
Samawa	34.8	111.0	77.1	18.88
Sinjar	24.5	101.9	66.3	19.79
Sulaymania	18.1	97.2	62.2	19.53
Telafer	25.4	104.7	68.3	19.63
Tikrit	30.2	108.7	72.6	18.86
	Relative humidity (%)			
	Min.	**Max.**	**Mean**	**SD**
Baghdad	16.57	91.85	36.02	19.13
Basra	16.61	94.45	32.53	19.37
Diwania	16.78	95.39	34.89	18.51
Dohuk	14.63	98.21	44.90	23.12
Erbil	15.40	94.66	41.07	21.24
Al-Hai	15.30	93.86	31.93	19.94
Hila	16.43	91.59	33.89	18.45
Karbalaa	19.00	90.93	36.97	17.06
khaniqen	14.82	92.30	36.50	20.32
Kirkuk	15.30	95.37	39.29	21.31
Mosul	14.67	95.45	42.36	22.51
Najaf	15.77	89.77	32.58	18.17
Nasirya	15.25	93.37	29.96	18.69
Nukhib	15.47	91.70	32.90	18.00
Ramadi	19.69	95.39	38.68	18.03
Rutba	17.05	93.55	35.24	18.28
Samawa	15.15	92.55	31.06	18.36
Sinjar	17.36	96.10	44.58	22.43
Sulaymania	15.87	98.00	44.62	22.95
Telafer	16.33	95.93	42.28	22.32
Tikrit	17.79	94.85	37.46	19.51

Standardized Temperature Index (STI)

The Standardized Temperature Index (STI) was used to evaluate the hot condition and was calculated in a similar way to the SPI [24]. The temperature data is first subjected to a gamma distribution and then converted to the standardized standard normal distribution. The STI indicates that a positive value corresponds to warmer temperatures, while a negative value indicates colder conditions. Table 2 summarized the STI classifications. A one-month timescale was used for the standardized temperature index to determine the monthly characteristics of temperatures throughout the year.

Table 2: HI and STI classifications.

Heat index	
Heat index range (°F)	**HI Classification**
< 80°F	Normal/Safe
80°F – 90°F	Caution
90°F – 103°F	Extreme Caution
103°F – 124°F	Danger
125°F or higher	Extreme Danger
Standardized temperature index	
STI Threshold	**STI Classification**
STI ≥ 2.5	Extreme Hot
1.5 ≤ STI < 2.5	Severe Hot
0.5 ≤ STI < 1.5	Mild Hot
0.0 ≤ STI < 0.5	Normal Hot
-0.5 ≤ STI < 0.0	Normal Cold
-1.5 ≤ STI < -0.5	Mild Cold
-2.5 ≤ STI < -1.5	Severe Cold
STI < -2.5	Extreme Cold

Gene Expression Programming (GEP)

GEP is an evolutionary algorithm that is structurally similar to genetic algorithm that developed by Candida Ferreira [25]. The GEP program has received increasing attention from the scientific community over the past few years, leading to an increase in its applications in various research fields. The GEP algorithm uses a fixed-length linear representation of computer programs, which is ultimately converted into an expression tree structure. Each genome, or chromosome, in this algorithm consists of a linear sequence of fixed-length codes, which can represent one or more genes. There are two main types of elements in GEP; functional elements and terminal elements. In a gene expression tree, genes consist of two elements: the head and the tail. The head contains the variables and constants, while the tail represents the functions. Using a programming language called Karva, the gene expression tree is developed in the GEP algorithm. Developing a gene expression programming model requires completing five initial steps. To start, we identify the independent variables that constitute the individual programs. Next, we defined the required mathematical operations for the expression. After identifying these components, the fitness function is determined by fixing the number of genes and the linking function. The last step involves specifying the genetic parameters. Figure 2 shows an example to present the gene consisting of head length 4 and tail length of

5, aimed at square root the expression ((a + b) * (x – y)). In this tree example, the head section is depicted in red, while the tail section is shown in blue. For further details about the GEP algorithm, refer to [25].

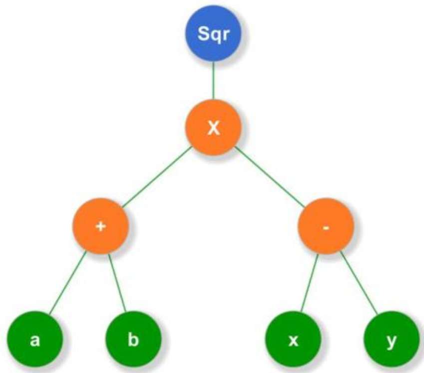

Figure 2: Expression tree diagram for the mathematical equation $\sqrt{(a+b)*(x-y)}$.

Results and Discussion

The heat index and the standardized temperature index were calculated across Iraq using a computer program developed using the Visual Basic programming language. The heat index data were analyzed in terms of spatial distribution and impact, as well as in terms of temporal distribution, using two-time scales: daily and monthly. Analysis of the daily heat index data for Iraq reveals that the majority, 62.4%, falls within the normal classification. while the caution classification constitutes 22.6%. The extreme caution classification constitutes 14%. It's worth noting that the danger classification is minimal, not exceeding 1%. Analysis of the monthly heat index shows that the percentage of classifications for the normal, caution and extreme caution were 62%, 22.3% and 15.7% respectively. Figure 3A shows the frequency of daily heat index classifications, while Figure 3B shows the frequency of monthly heat index classifications for each of the meteorological stations under study. The spatial analysis of heat index classifications in Iraq, as shown in Figure 4, indicates that the northern region has a higher percentage of the “normal” classification when compared to the central and southern regions. Notably the western area records the highest percentage of the "caution" classification, while the northern and southern regions show lower. This trend can be attributed to the elevated humidity levels in the southern and northern regions, contrasting with the drier climate prevalent in the western region, which is influenced by its desert conditions. Furthermore, the analysis reveals that the northern and western parts of Iraq report a lower incidence of the “extreme caution” classification, while the southern region stands out with the highest frequency. This variation is linked to the high temperatures experienced in the southern regions, especially during the months of July and August.

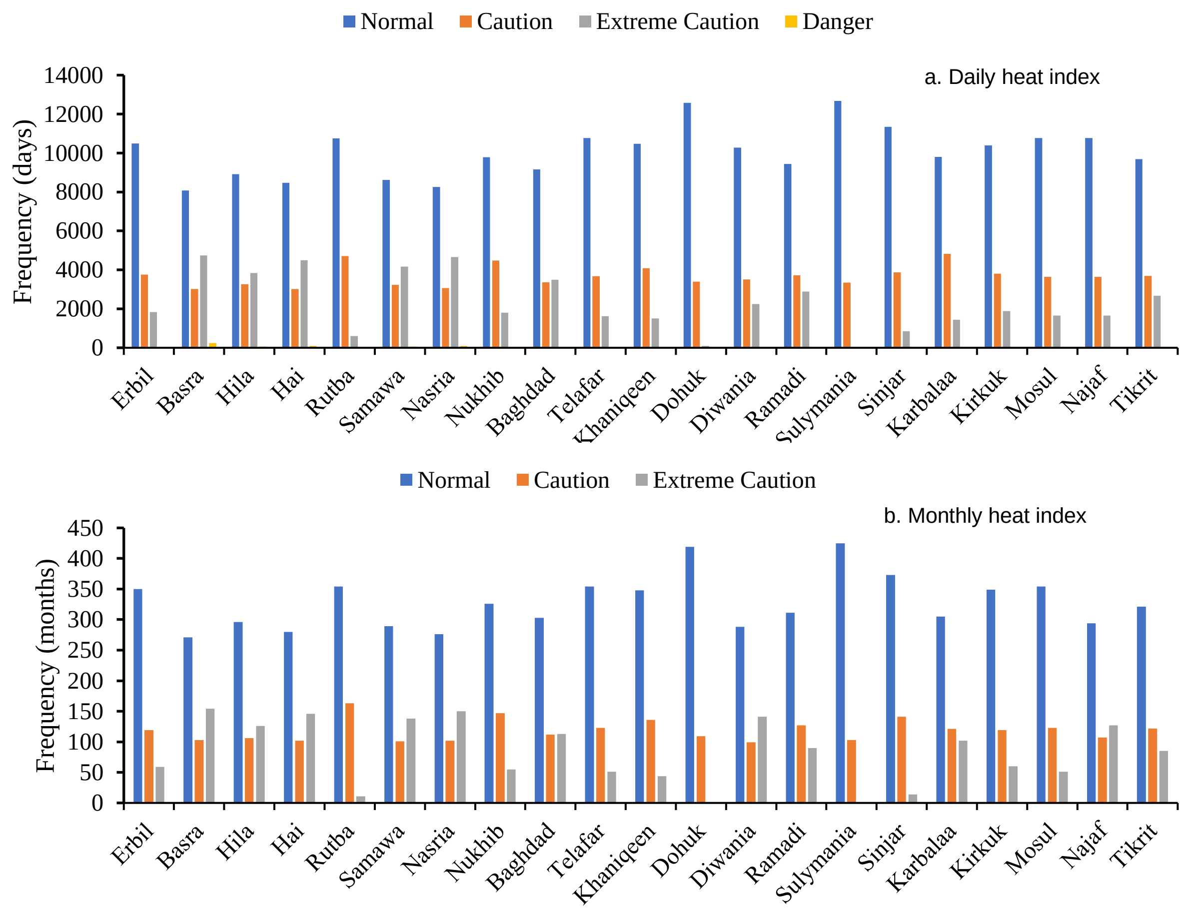

Figure 3: Frequency of daily and monthly heat index classifications for meteorological stations under study.

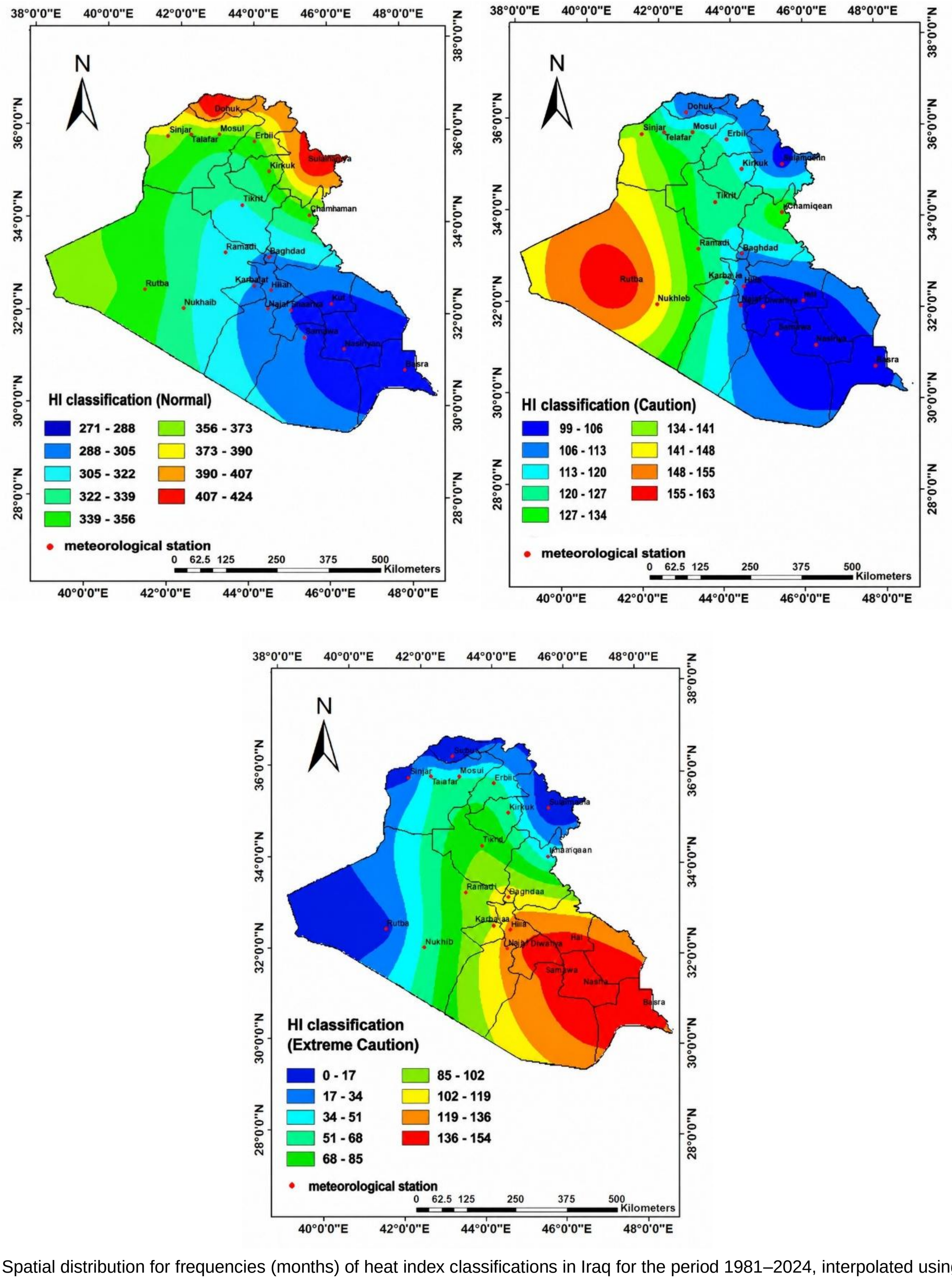

Figure 4. Spatial distribution for frequencies (months) of heat index classifications in Iraq for the period 1981–2024, interpolated using the kriging method.

The Mann-Kendall test was used to analyze the trend of the heat index. The results of this test, conducted at all the meteorological stations used, indicate a significant upward trend in the heat index at a subset of stations. The Sen's slope test was used to estimate the slope of the time series trend of the heat index. Time series analysis of the heat index using the Sen's slope test for all studied meteorological stations showed that the slope of the heat index series in stations located in northern Iraq ranged between 0.085 and 0.102 °F per year, while in stations located in the central region it ranged between 0.071 and 0.090 °F per year, and in stations located in the southern region it ranged between 0.068 and 0.078 °F per year. Table 3 summarizes the results of the Sen's slope test for all meteorological stations under study. Northern Iraq is warming at a faster rate Sen's slope 0.096 and 0.108 °F per year, but southern Iraq still records the highest absolute frequency of "extreme caution" classifications (Figure 4). This is attributed to the extreme temperatures that northern Iraq has begun to experience as a result of climate change, in addition to the decrease in relative humidity levels. By analyzing the Sen's slope results, it is evident that northern Iraq is warming faster (steeper Sen's slope), whereas southern Iraq remains the hotter region in absolute terms.

Table 3. results of the Sen's slope test (°F per year) for all meteorological stations under study.

Station name	Kendall's tau	p-values	Sen's slope
Sulymania	0.051	0.080	0.0852
Erbil	0.053	0.068	0.0948
Dohuk	0.058	0.048	0.0984
Kirkuk	0.050	0.084	0.0900
Mosul	0.057	0.049	0.1020
Telafar	0.055	0.060	0.0972
Sinjar	0.057	0.052	0.0984
Tikrit	0.050	0.084	0.0900
Ramadi	0.050	0.086	0.0900
Rutba	0.051	0.081	0.0792
Baghdad	0.045	0.119	0.0804
Khaniqeen	0.046	0.118	0.0768
Hila	0.042	0.145	0.0744
Hai	0.042	0.151	0.0708
Karbalaa	0.045	0.121	0.0816
Najaf	0.041	0.154	0.0720
Samawa	0.041	0.160	0.0684
Diwania	0.041	0.157	0.0708
Nasria	0.041	0.157	0.0708
Basra	0.045	0.122	0.0732
Nukhib	0.048	0.098	0.0780

By analyzing the temperature series trend of all the meteorological stations under study using the Mann-Kendall test, it was found that all the stations under study had an upward trend that is statistically significant only at a subset of stations, primarily in the north. Analysis of the relative humidity series trend for all the meteorological stations under study using the Mann-Kendall test showed that all the stations under study had a downward trend with a slope ranging from -0.001 to -0.002 according to the Sen's slope test.

Analysis of the standardized temperature index in Iraq reveals some interesting insights. The data shows that severe hot classifications account for 2% of the total STI classifications, while Mild hot classifications make up 36.3%. Normal hot classifications represent 14.2%, with normal cold classifications at 8%, mild cold at 36.2%, and severe cold at 3.3%. Notably, Mild cold and mild hot classifications form the largest segments of the STI classifications throughout the year. Figure 5 shows the frequency of STI classifications for all meteorological stations under study.

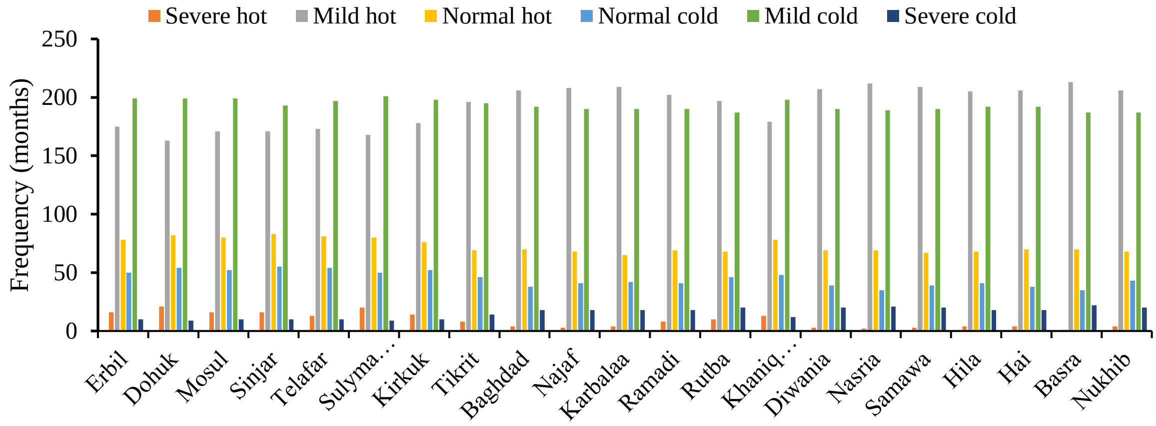

Figure 5. frequency of STI classifications for all meteorological stations under study.

Analyzing the spatial distribution of the STI in Iraq, as illustrated in Figure 6, reveals that the normal cold classification occurs more often in the northern region compared to the central and southern regions. and this classification is noticeably less frequent in the southern part of the country. It was observed that the northern region of the country exhibited a greater prevalence of the normal hot classification of STI when compared to the central and southern regions. Analysis of the mild cold classification shows that this classification was more common in northern Iraq compared to central and southern Iraq, while the mild hot classification was more common in southern Iraq compared to the north. This is one of the characteristics of Iraq's climate. Analysis of the STI classification of severe cold shows that it was more frequent in southern Iraq and less frequent in the north, while severe hot classifications were more common in northern Iraq than in the south. This, logically, contradicts the usual climatic characteristics of Iraq, which is typically colder in its northern regions than in its southern regions. Nevertheless, recent years have witnessed unprecedented high temperatures in northern Iraq and unprecedented low temperatures in the south. This is attributed to climate change, which is impacting Iraq.

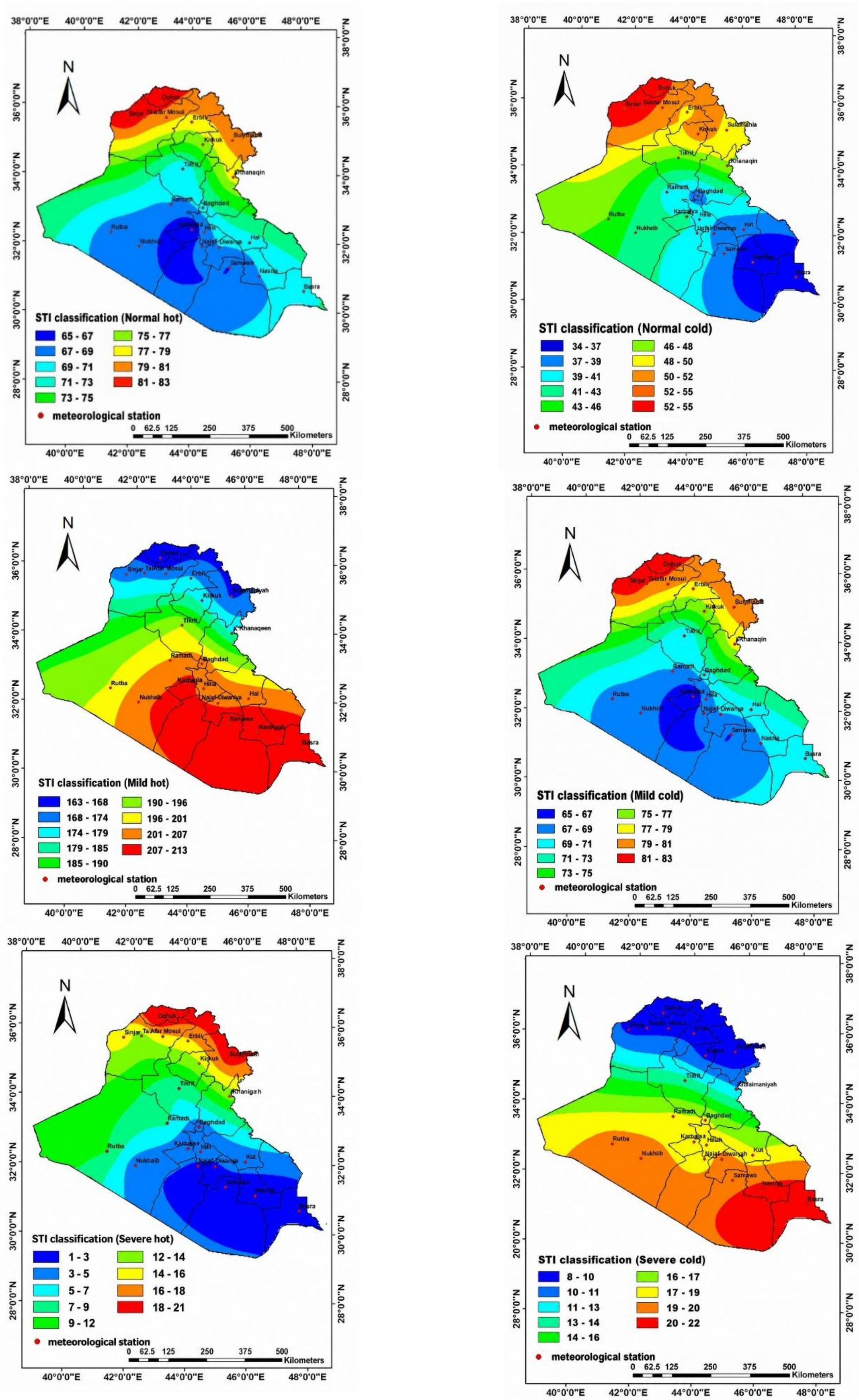

Figure 6. Spatial distribution for frequencies (months) of STI classifications in Iraq for the period 1981–2024, interpolated using the kriging method.

By comparing the STI and HI indices, we note that both indices are used to measure heat conditions but with different objectives: the STI is a statistical measure to compare temperature against the historical series of temperatures for the same meteorological station, while the HI measures the immediate physiological stress caused by air temperature and humidity. Analysis of the two indices shows that temperatures in Iraq are still within acceptable ranges for human tolerance, and relative humidity plays a pivotal role in mitigating the impact of extreme temperatures on humans.

The GEP algorithm was used to develop a mathematical equation to facilitate the steps for calculating the heat index in Iraq and to obtain a simpler mathematical equation for estimating the heat index in Iraq. Daily heat index data were analyzed using a GEP algorithm. The data were divided into two sets: 80% for model training and 20% for model validation.

Equation 5 illustrates the mathematical expression developed using the GEP algorithm with a coefficient of determination (R^2) 0.99, Root Mean Squared Error (RMSE = 1.101, Mean Squared Error (MSE = 1.213), Mean Absolute Error (MAE = 0.877), and Mean Absolute Percentage Error (MAPE = 1.334) in the training phase and R^2 = 0.98, RMSE = 1.104, MSE = 1.390, MAE = 0.958, and MAPE = 1.338 in the testing phase to estimate HI in Iraq. Table 4 summarizes the GEP settings used to develop equation 5. The equation can be used for all ranges of mean daily temperature and relative humidity values recorded in Iraq. The equation was trained over the (T, RH) envelope of approximately T = 15.1 to 111.81 °F and RH = 14 to 98%. The equation is an empirical relationship with no dimensions, and the coefficients are not physical.

$$HI = (T + 2.098(RH)^{0.25} + (RH + T)^{0.375}) - 10.935 \qquad (5)$$

Where, HI = heat index in Fahrenheit, RH = relative humidity in (%), and T = temperature in Fahrenheit.

Table 4: GEP setting

Function set	+, -, *, /, power
General	
Population size	50
Genes per chromosomes	8
Gene head length	16
Fitness function	MAE
Linking function	Addition
Genetic operators	
Mutation rate	0.044
Inversion rate	0.1
Gene transportation rate	0.1
Gene recombination rate	0.3

Figure 7 shows the scatter plot of the Heat index (estimated by NWS) versus the Heat index (estimated by GEP Equation 5) for the test set. The scatter plot in Figure 7 demonstrates the efficiency of Equation 5, as most of the data fall within the 1:1 line.

Limitation

This study is subject to several limitations that should be acknowledged. First, meteorological variables were obtained from the NASA POWER satellite-based meteorological dataset rather than in situ observations. Although NASA POWER provides spatially and temporally consistent fields, it remains an indirect estimate that may deviate from ground-based measurements at some locations and time periods, particularly in regions with complex terrain or sparse station coverage. These uncertainties can propagate into the calculated heat index and standardized temperature index values. Second, we relied on mean daily and monthly air temperature to compute the heat index, instead of using maximum temperature or sub-daily extremes. The use of mean values provides a robust indicator of general heat conditions but likely underestimates short-lived peak heat stress events, such as afternoon heat spikes or multi-hour heat waves, that are critical from a human health perspective. Future work should therefore incorporate maximum and/or high-frequency temperature data to better capture these extremes. Third, the spatial patterns presented in the GIS maps depend on the kriging interpolation approach and the distribution of the 21 station locations. Kriging assumes spatial autocorrelation and relatively smooth variation between sampled points and may not fully resolve local-scale heterogeneity arising from land use, topography, or urban heat-island effects. As a result, fine-scale hotspots or cool spots may not be represented accurately on the maps. Increasing station density, testing alternative interpolation schemes, and combining satellite-based land-surface information could improve the robustness of the spatial analysis in future studies.

Despite these limitations, the consistency of the trends across stations and time scales supports the main conclusion that heat stress is increasing in Iraq and that northern regions are becoming more exposed to extreme heat conditions under ongoing climate change.

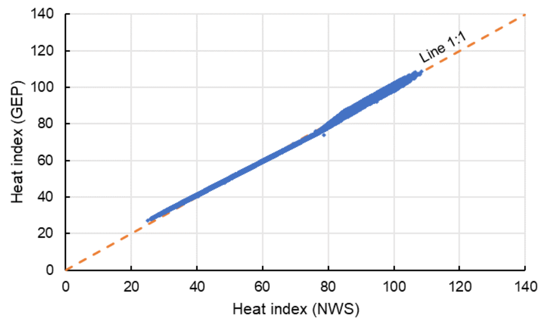

Figure 7. HI (estimated by NWS)-vs-HI (estimated by GEP Eq. 5) scatter plot for the test set

Conclusion

The study demonstrated the feasibility of using a daily heat index in Iraq, utilizing temperature and relative humidity data from NASA POWER (Prediction Of Worldwide Energy Resources). Furthermore, using the daily average of temperature and relative humidity contributes to calculating the average daily heat index for climate analysis, which helps identify the effects of climate change in the study area. This represents an innovative approach to calculating heat index values, which previously relied on the highest temperature of the day, yielding results for the hottest times of day for purely medical purposes. This opens new avenues for further research in this field.

The study demonstrated the efficiency of a gene expression programming algorithm in developing mathematical equations with easily applicable expression formulas for calculating the daily heat index in the study area. The researchers recommend conducting a study to predict daily heat index values using data derived from climate change models, in order to determine the values of this index for the period from 2026 to 2100 in Iraq, and to assess future changes in heat stress levels.

Disclosure Statement

Ethics approval and consent to participate

Not applicable

Consent for publication

Not applicable

Declarations

This study is not derived from any thesis or dissertation.

Availability of data and materials

The raw data required to reproduce these findings are available within the body of this manuscript and its accompanying figures and tables.

Author's contribution

The author confirms contribution to the paper as follows: study conception and design, theoretical calculations and GEP modeling: Anas Mahmood Al-Juboori; data analysis and validation, and manuscript preparation: Mustafa S. Mustafa; Preparing maps using GIS: Basma A.M. Al-Jawadi. All authors reviewed the results and approved the final version of the manuscript.

Funding

This research received no specific grant from any funding agency in the public, commercial, or not-for-profit sectors.

Conflicts of interest

The authors declare that there is no conflict of interest regarding the publication of this article.

Acknowledgements

The authors acknowledge the NASA POWER project for providing the meteorological data used in this study

Open Access

References

[1] IPCC. Weather and Climate Extreme Events in a Changing Climate. Climate Change 2021 – The Physical Science Basis, Cambridge University Press; 2023, p. 1513–766. https://doi.org/10.1017/9781009157896.013.

[2] Ebi KL, Capon A, Berry P, Broderick C, de Dear R, Havenith G, et al. Hot weather and heat extremes: health risks. The Lancet 2021;398:698–708. https://doi.org/10.1016/S0140-6736(21)01208-3.

[3] Essa W, Lhissou R. Downscaling of Thermal Images Over the Gaza Strip Using the Land Surface Temperature—Spectral Indices Relation: Case Study; Hot, Arid, and Semi-Arid Areas. An-Najah University Journal for Research - A (Natural Sciences) 2023;37:7–24. https://doi.org/10.35552/anujr.a.37.2.2103.

[4] Wang S, Sun QC, Huang X, Tao Y, Dong C, Das S, et al. Health-integrated heat risk assessment in Australian cities. Environ Impact Assess Rev 2023;102:107176. https://doi.org/10.1016/j.eiar.2023.107176.

[5] Munasinghe L, Jun T, Rind DH. Climate change: a new metric to measure changes in the frequency of extreme temperatures using record data. Clim Change 2012;113:1001–24. https://doi.org/10.1007/s10584-011-0370-8.

[6] Havenith G, Fiala D. Thermal Indices and Thermophysiological Modeling for Heat Stress. Compr Physiol 2016;6:255–302. https://doi.org/10.1002/j.2040-4603.2016.tb00668.x.

[7] Cramer MN, Gagnon D, Laitano O, Crandall CG. Human temperature regulation under heat stress in health, disease, and injury. Physiol Rev 2022;102:1907–89. https://doi.org/10.1152/physrev.00047.2021.

[8] Abdul-Nabi SS, Al Karaki V, Khalil A, El Zahran T. Climate change and its environmental and health effects from 2015 to 2022: A scoping review. Heliyon 2025;11:e42315. https://doi.org/10.1016/j.heliyon.2025.e42315.

[9] Adamo N, Al-Ansari N, Sissakian V, Fahmi KJ, Abed SA. Climate Change: Droughts and Increasing Desertification in the Middle East, with Special Reference to Iraq. Engineering 2022;14:235–73. https://doi.org/10.4236/eng.2022.147021.

[10] Zhou Z, Nguyen-Xuan T, Liao H, Qiu L, Im E-S. Characterization of temperature and humidity effects on extreme heat stress under global warming and urban growth in the Pearl and Yangtze River Deltas of China. Weather Clim Extrem 2024;44:100659. https://doi.org/10.1016/j.wace.2024.100659.

[11] Rachid A, Qureshi AM. Sensitivity Analysis of Heat Stress Indices. Climate 2023;11:181. https://doi.org/10.3390/cli11090181.

[12] Alvarez I, Diaz-Poso A, Lorenzo MN, Roye D. Heat index historical trends and projections due to climate change in the Mediterranean basin based on CMIP6. Atmos Res 2024;308:107512. https://doi.org/10.1016/j.atmosres.2024.107512.

[13] Guo Y, Wu Z, Zheng Z, Huang X, Hu Z. Summer Thermal Comfort Zoning Studies of Mainland China Based on the Comprehensive Heat Index. International Journal of Climatology 2025;45. https://doi.org/10.1002/joc.70035.

[14] Hoang TLT, Dao HN, Cu PT, Tran VTT, Tong TP, Hoang ST, et al. Assessing heat index changes in the context of climate change: A case study of Hanoi (Vietnam). Front Earth Sci (Lausanne) 2022;10. https://doi.org/10.3389/feart.2022.897601.

[15] Perkins SE, Alexander L V., Nairn JR. Increasing frequency, intensity and duration of observed global heatwaves and warm spells. Geophys Res Lett 2012;39. https://doi.org/10.1029/2012GL053361.

[16] Russo S, Sillmann J, Sterl A. Humid heat waves at different warming levels. Sci Rep 2017;7:7477. https://doi.org/10.1038/s41598-017-07536-7.

[17] Zhou Z, Zhang L, Zhang Q, Hu C, Wang G, She D, et al. Global increase in future compound heat stress-heavy precipitation hazards and associated socio-ecosystem risks. NPJ Clim Atmos Sci 2024;7:33. https://doi.org/10.1038/s41612-024-00579-4.

[18] Brimicombe C, Lo CHB, Pappenberger F, Di Napoli C, Maciel P, Quintino T, et al. Wet Bulb Globe Temperature: Indicating

Extreme Heat Risk on a Global Grid. Geohealth 2023;7. https://doi.org/10.1029/2022GH000701.

[19] Hamed MM, Kyaw AK, Nashwan MS, Shahid S. Spatiotemporal changes in Universal Thermal Climate Index in the Middle East and North Africa. Atmos Res 2023;295:107008. https://doi.org/10.1016/j.atmosres.2023.107008.

[20] Sissakian VK, Adamo N, Al-Ansari N. The Severe Consequences of Climate Change in Iraq: A Case Study. Engineering 2023;15:242–60. https://doi.org/10.4236/eng.2023.154019.

[21] Zittis G, Almazroui M, Alpert P, Ciais P, Cramer W, Dahdal Y, et al. Climate Change and Weather Extremes in the Eastern Mediterranean and Middle East. Reviews of Geophysics 2022;60. https://doi.org/10.1029/2021RG000762.

[22] NASA POWER Project. Prediction Of Worldwide Energy Resources (POWER) Data Access Viewer, Global Meteorology (Climatology and Daily), Release 4, NASA Langley Research Center, Hampton, VA, USA. Available from: https://power.larc.nasa.gov/data-access-viewer/

[23] Al-Maliki LA, Al-Mamoori SK, El Tawil K, Al-Ansari N, Comair FG. Assessing the Accuracy of NASA Power Meteorological Data in Iraq. Tikrit Journal of Engineering Sciences 2025;32:1–23. https://doi.org/10.25130/tjes.32.4.12.

[24] Thomas B. McKee, Nolan J. Doesken, John Kleist. The relationship of drought frequency and duration to time scales. Eighth Conference on Applied Climatology, California: 1993. https://www.jstor.org/stable/26230365

[25] Candida Ferreira. Gene expression programming: a new adaptive algorithm for solving problems. Complex Systems 2001;13:87–129. https://arxiv.org/abs/cs/0102027